Simplified Cannonball Trajectory Model

Team No. 264

Problem B: Artillery

November 9, 2025

Abstract

This study presents a systematic analysis and modeling of the ballistic characteristics of typical 19th-century artillery. The research focuses on three main aspects:

(1) **Development of a two-dimensional ballistic model** considering air resistance and altitude variation. By accounting for the change of air density with altitude and the Reynolds-number-dependent drag coefficient, the projectile motion equations were solved using the fourth-order Runge–Kutta method. Under calm-air conditions, the minimum launch velocity was found to be 117.55 m/s with an optimal elevation angle of 43.5°. Compared with the ideal vacuum model (108.5 m/s, 45°), air resistance slightly reduces the optimal angle and increases the required launch velocity by approximately 8.3%, demonstrating its significant impact on range and stability.

(2) **Construction of a three-dimensional ballistic model** incorporating wind field and terrain elevation effects. The model describes projectile motion under varying wind components, horizontal distances, and target altitudes, analyzing the corresponding minimum initial velocity and optimal launch angle for headwind, tailwind, and crosswind conditions. Numerical simulations confirmed that the vertical wind component can be neglected with negligible error, enabling a substantial simplification of the model. Based on this, a semi-empirical formula suitable for manual estimation by historical artillery officers was derived, linking wind speed, wind direction, terrain elevation difference, and horizontal distance with the launch parameters.

Keywords: artillery ballistics; aerodynamic drag; wind effects; multivariate regression; numerical simulation

Contents

1 Problem Analysis

1.1 Introduction

The nineteenth to early twentieth century marked a crucial period in the rapid development of modern artillery technology[1]. With the advancement of smokeless powder and the widespread adoption of metal breech-loading guns, significant progress was achieved in firing range, accuracy, and structural design. However, during this era, ballistic calculations still relied primarily on empirical formulas and idealized projectile models under highly limited computational conditions. Early ballistic theories commonly neglected air resistance and wind effects, estimating the relationship between range and launch angle using simplified parabolic equations.

By the mid-nineteenth century, scientists and military engineers gradually recognized the substantial influence of aerodynamic drag, air density variation, and wind fields on projectile trajectories. Consequently, various correction theories and empirical firing tables were developed, yet their construction remained complex and difficult to apply rapidly under field conditions[2].

In this study, a representative nineteenth-century cannon is investigated. The weapon fires a 5 kg spherical projectile with a diameter of 11 cm and a maximum muzzle velocity of 450 m/s. Under these conditions, the impact requirements for targets at different horizontal ranges and altitudes are analyzed. By incorporating wind speed and direction into the aerodynamic resistance model, a modified ballistic dynamic system is established. Numerical simulations and clustering methods are then employed to determine the minimal required muzzle velocity and corresponding launch angle under varying wind conditions. The objective is to develop a simplified estimation approach that enables mathematically trained artillery officers—without access to computational tools—to rapidly determine appropriate firing parameters from pre-calculated tables, thereby improving historical firing accuracy and operational efficiency.

This research not only provides insight into how environmental factors constrained nineteenth-century artillery performance but also offers a quantitative reference for reconstructing early ballistic computation methods and understanding the evolution of empirical firing theory.

1.2 Problem Analysis

This paper addresses the problem of determining firing parameters for a classic spherical projectile cannon from 150–200 years ago (projectile mass 5 kg, diameter 11 cm, maximum muzzle velocity 450 m/s). The study is organized around two complementary objectives—accurate analysis of baseline conditions and construction of a practical estimation method—so as to balance historical weapon characteristics with operational usability.

First, a high-fidelity model is developed for the idealized baseline scenario: the cannon and target are located at the same altitude of 500 m, the horizontal range is 1200 m, and wind effects are neglected. The projectile's forces are thereby limited to gravity acting vertically downward and aerodynamic drag opposing the instantaneous velocity. Because muzzle velocities for this class of cannon lie in a relatively high-speed regime and the projectile is spherical, simple drag models are insufficient to capture the relevant aerodynamics. Accordingly, the drag law is modified to reflect the aerodynamic properties of a sphere, and the resulting corrected drag term is incorporated into the two-dimensional equations of motion. The required muzzle velocity and corresponding horizontal launch angle that satisfy the hit condition are obtained by numerical integration of these governing differential equations.

Building on this baseline, the analysis is extended to more realistic operational conditions: horizontal ranges from 1000 m to 1500 m, nonzero altitude differences between cannon and target, and varying wind speeds and directions. The wind field is decomposed into components along the projectile's horizontal and vertical directions to quantify its effect on the projectile's air-relative velocity; this, in turn, modifies both the magnitude and direction of aerodynamic drag. The complete equations of motion—including gravity and the corrected aerodynamic drag—are thus formulated and solved by an explicit Euler integration scheme. Guided by the operational objective of conserving materiel, the study focuses on the minimal muzzle velocity and its associated launch angle that achieve a hit, thereby ensuring that the solutions are both tactically sensible and resource-efficient.

Finally, to accommodate historical battlefield conditions where no computers or calculators are available, a rapid-estimation procedure suitable for mathematically trained artillery officers is developed. Using the numerical solver described above, a dataset of randomized scenarios is generated, sampling the key parameters: horizontal distance (1000–1500 m), altitude difference, wind speed, and wind direction. Nonlinear regression techniques are then used to derive analytic expressions relating launch angle and minimal muzzle velocity to the input parameters. The resulting formulae are validated against the baseline (equal-altitude, 1200 m, no-wind) case and distilled into concise, hand-computable estimation models that support rapid decision-making in the field.

2 Assumptions and Symbols

2.1 Model Assumptions

- The projectile surface is smooth.
- The influence of crosswind on the projectile's tumbling or yaw is neglected.
- Air flow is assumed to be steady and incompressible within the projectile's flight altitude range (500–2000 m).
- Gravitational acceleration is treated as a constant ($g = 9.80665\,\mathrm{m/s^2}$) since the altitude variation is small compared to the Earth's radius.

2.2 Notations

Symbol	Definition	Unit
m	Mass of the spherical projectile	kg
L	Horizontal distance between the cannon and target	m
h_0	Altitude of the cannon	m
h_t	Altitude of the target	m
z	Altitude difference	m
h_{eff}	Effective flight altitude ($h_{\text{eff}} = (h_0 + h_t)/2$)	m
v_0	Muzzle velocity	$\mathrm{m\,s^{-1}}$
θ	Firing elevation angle	$^\circ$
v	Velocity components	$\mathrm{m\,s^{-1}}$
$\vec{W}$	Wind velocity vector	$\mathrm{m\,s^{-1}}$
ϕ	Wind direction angle (relative to x-axis)	$^\circ$
ρ	Air density	$\mathrm{kg/m^3}$
ν	Kinematic viscosity of air	$\mathrm{m^2/s}$
T_0	Sea-level standard temperature (ISA model)	K
p_0	Sea-level standard pressure (ISA model)	Pa
L_b	Temperature lapse rate (ISA model)	$\mathrm{K\,m^{-1}}$
R	Specific gas constant for dry air	$\mathrm{J/(kg \cdot K)}$
F_ρ	Air density correction factor	Dimensionless
β	Empirical coefficient for density correction	Dimensionless

Table 1: Definition of key symbols and their units

3 Task 1

3.1 Model Establishment

In Task 1, we focus on a cannon deployed at an altitude of $h_0 = 500\,\text{m}$, with a target located at the same elevation and a horizontal distance of $L = 1200\,\text{m}$. The objective is to determine the required initial velocity and corresponding launch angle that ensure the projectile hits the target.

In this scenario, wind effects are neglected. The projectile is subjected to two dominant forces during its flight: gravity $\vec{G} = -mg\,\hat{y}$ and aerodynamic drag $\vec{F}_D = -\frac{1}{2}C_D\rho(h)Av\vec{v}$. The trajectory and corresponding force analysis are illustrated in Fig. 1.

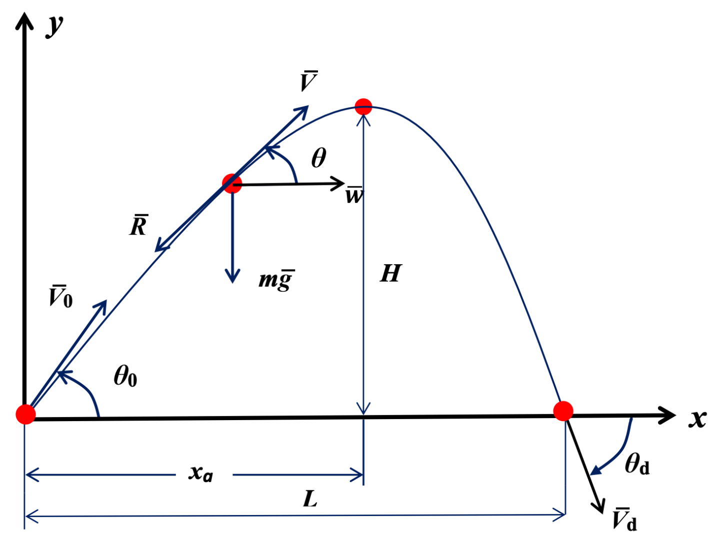

Figure 1: Diagram of force analysis

Accordingly, the equations of motion can be expressed as:

$$\begin{cases} m\dfrac{dv_x}{dt} = -\frac{1}{2}C_D\rho(h)Avv_x, \\ m\dfrac{dv_y}{dt} = -mg - \frac{1}{2}C_D\rho(h)Avv_y, \\ \dfrac{dx}{dt} = v_x, \quad \dfrac{dy}{dt} = v_y, \end{cases} \tag{1}$$

where $v = \sqrt{v_x^2 + v_y^2}$ denotes the magnitude of the velocity vector.

3.2 Formula Derivation

Since the projectile undergoes significant variations in vertical position and velocity during flight, both the drag coefficient C_D and air density $\rho(h)$ vary with Reynolds number

Re and altitude h, respectively. Therefore, a refined aerodynamic model is established to enhance computational accuracy.

3.2.1 Air Density Model

The air density is computed using the International Standard Atmosphere (ISA) model for the troposphere, which applies for $h \leq 11\,\mathrm{km}$:

$$\rho(h) = \frac{p_0}{RT_0}\left(1 - \frac{L_b h}{T_0}\right)^{\frac{g_0}{RL_b}-1}, \tag{2}$$

where parameters are determined based on ISA data and literature: $T_0 = 288.15\,\mathrm{K}$ (sea-level standard temperature), $p_0 = 101325\,\mathrm{Pa}$ (sea-level pressure), $L_b = 0.0065\,\mathrm{K/m}$ (temperature lapse rate), $R = 287.05\,\mathrm{J/(kg \cdot K)}$ (specific gas constant for dry air), and $g_0 = 9.80665\,\mathrm{m/s^2}$ (gravitational acceleration at sea level).

3.2.2 Drag Coefficient Model

The Reynolds number is defined as $\mathrm{Re} = \dfrac{vD}{\nu}$, where $D = 0.11\,\mathrm{m}$ is the projectile diameter and $\nu = 1.5 \times 10^{-5}\,\mathrm{m^2/s}$ is the kinematic viscosity of air under standard conditions.

For a spherical projectile, Morrison et al. [3] proposed a widely accepted empirical correlation between C_D and Re:

$$C_D = \frac{24}{Re} + \frac{2.6\left(\frac{Re}{5.0}\right)}{1+\left(\frac{Re}{5.0}\right)^{1.52}} + \frac{0.411\left(\frac{Re}{2.63\times 10^5}\right)^{-7.94}}{1+\left(\frac{Re}{2.63\times 10^5}\right)^{-8.00}} + \frac{0.25\left(\frac{Re}{10^6}\right)}{1+\left(\frac{Re}{10^6}\right)}. \tag{3}$$

However, this expression is only valid for $\mathrm{Re} < 10^6$. Given the maximum muzzle velocity $v_0 = 450\,\mathrm{m/s}$, the corresponding Reynolds number is $\mathrm{Re} = 7.72 \times 10^6$, which exceeds the valid range.

To address this, we referred to the drag characteristics of spherical bodies in the transonic and supersonic regimes (see Fig. 2) and integrated empirical relations from related studies to construct a piecewise definition for $C_D(\mathrm{Re})$:

$$C_D(Re) \approx \begin{cases} \dfrac{24}{Re} + \dfrac{2.6\left(\frac{Re}{5.0}\right)}{1+\left(\frac{Re}{5.0}\right)^{1.52}} + \dfrac{0.411\left(\frac{Re}{2.63\times 10^5}\right)^{-7.94}}{1+\left(\frac{Re}{2.63\times 10^5}\right)^{-8.00}} + \dfrac{0.25\left(\frac{Re}{10^6}\right)}{1+\left(\frac{Re}{10^6}\right)}, & Re \leq 10^6, \\ 0.145 + 0.04\log_{10}\left(\dfrac{Re}{10^6}\right), & 10^6 < Re \leq 3\times 10^7, \\ 0.20, & Re > 3\times 10^7. \end{cases} \tag{4}$$

To validate the accuracy of Eq. (4), the fitted curve was compared with the NASA experimental dataset [4], showing strong consistency. Therefore, this model is adopted in subsequent calculations.

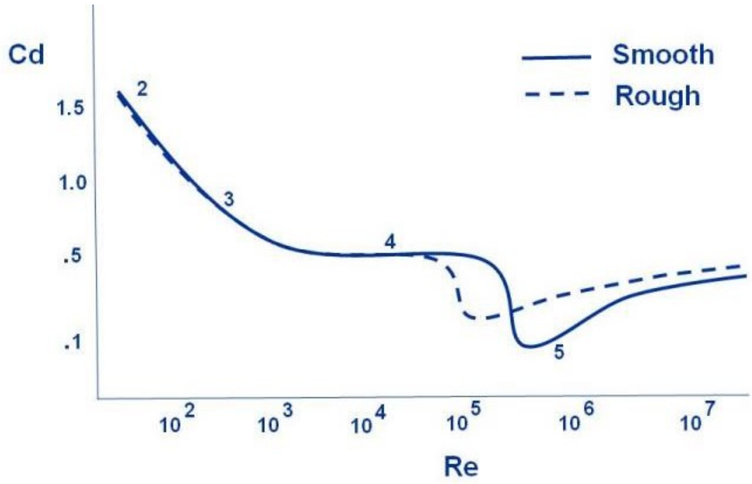

Figure 2: Variation of C_D with Reynolds number

In the ideal (drag-free) case, the minimum required velocity is $v_{0,\min} = 108.5\,\mathrm{m/s}$, corresponding to $\mathrm{Re} = 7.72 \times 10^5$ and $C_D = 0.11$. At $v_{0,\max} = 450\,\mathrm{m/s}$, C_D increases to 0.16. Since C_D varies slowly within this interval (as observed in Fig. 2), we approximate its mean value by the mean-value theorem of integration, obtaining $C_D \approx 0.15$. This value is adopted for subsequent numerical computations.

Substituting the refined expressions into Eq. (1), we derive the final simplified form of the motion equations:

$$\begin{cases} \dfrac{dv_x}{dt} = -\dfrac{C_D(\mathrm{Re}) \cdot \rho(h) \cdot A \cdot \sqrt{v_x^2 + v_y^2} \cdot v_x}{2m}, \\ \dfrac{dv_y}{dt} = -g - \dfrac{C_D(\mathrm{Re}) \cdot \rho(h) \cdot A \cdot \sqrt{v_x^2 + v_y^2} \cdot v_y}{2m}, \\ \dfrac{dx}{dt} = v_x, \\ \dfrac{dy}{dt} = v_y, \end{cases} \tag{5}$$

where $v = \sqrt{v_x^2 + v_y^2}$ represents the projectile speed, and $(x(t), y(t))$ denote its horizontal and vertical coordinates, respectively.

3.3 Numerical Solution

Given the strong nonlinearity of Eq. (5), an analytical solution is not feasible. We thus employ the fourth-order Runge–Kutta method with a time step of $\Delta t = 0.02\,\mathrm{s}$ to numerically integrate Eq. (1). At each time step, the air density $\rho(h)$ and drag coefficient $C_D(v)$

are updated based on the current state. Integration terminates when $y(t) < 0$, indicating that the projectile has reached the ground. The corresponding horizontal displacement x_{impact} is then recorded.

For each launch angle θ, a binary search is used to determine the minimum initial velocity v_0 satisfying:

$$x_{\text{impact}}(v_0, \theta, h_0) = L, \tag{6}$$

where a tolerance of $|x_{\text{impact}} - L| < 0.05\,\text{m}$ is used to denote a successful hit.

By scanning $\theta \in [2°, 88°]$, we obtain the complete relationship between the launch angle and the minimum required initial velocity, as illustrated in Fig. 3.

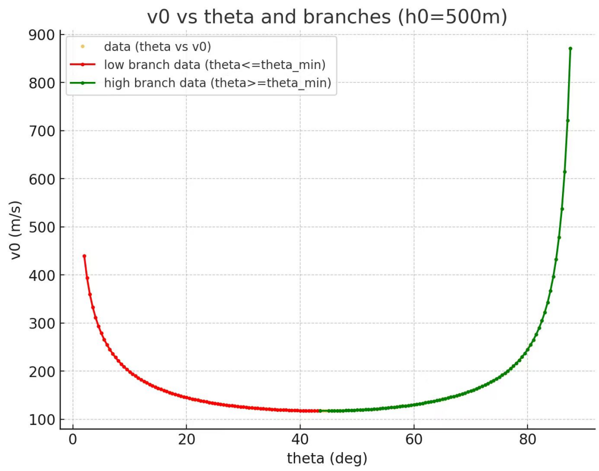

Figure 3: Relationship between initial velocity V_0 and launch angle θ

As shown, the function $v_0(\theta)$ exhibits a characteristic U-shaped distribution: at small angles, longer flight times lead to greater drag loss, while at large angles, excessive vertical components increase gravitational energy loss. The minimum value occurs near $\theta = 43.5°$, yielding:

$$v_{0,\min} = 117.55\,\text{m/s}.$$

The corresponding trajectory and parameter variations at this condition are shown in Fig. 4.

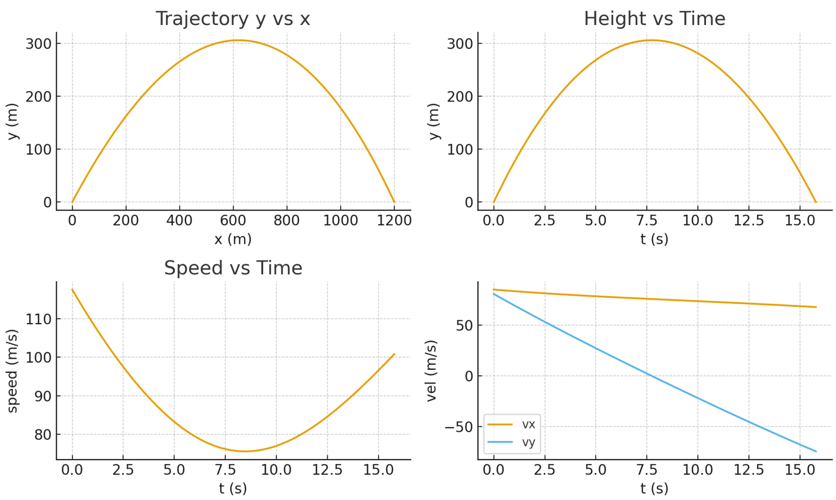

Figure 4: Trajectory and dynamic variation at $v_{0,\text{min}} = 117.55\,\text{m/s}$

Table 2 lists selected results for different launch angles:

Table 2: Minimum initial velocity at different launch angles

θ (°)	10	20	30	43.5	60
v_0 (m/s)	195.4	134.5	120.7	**117.6**	134.2

Compared with the ideal (drag-free) projectile motion, the minimum initial velocity increases from 108.5 m/s to 117.5 m/s, approximately an 8.3% rise. The gradual decrease of air density with altitude slightly reduces drag during the ascent phase, extending the overall range. As a result, the optimal launch angle shifts from 45° (ideal case) to 43.5°, indicating that aerodynamic drag tends to lower the angle corresponding to maximum range.

Therefore, considering altitude-dependent air density and realistic aerodynamic drag, the final results are:

$$\boxed{v_{0,\text{min}} = 117.55\,\text{m/s}, \quad \theta_{\text{min}} = 43.5^\circ.}$$

4 Task 2

4.1 Model Development

Compared with the idealized conditions in Task 1, Task 2 requires consideration of varying wind directions and speeds. In addition, the target's horizontal distance is extended to the 1000–1500 m range, and the altitudes of the gun and target may differ. Based on classical exterior ballistics theory, the wind field primarily affects the projectile by altering its velocity relative to the air, thereby changing the magnitude and direction of aerodynamic drag. Consequently, the original two-dimensional model must be extended into three-dimensional space for further analysis.

To quantify the modeling parameters, the following coordinate system is established: the x-axis is defined along the horizontal line from the gun to the target (positive toward the target), the z-axis is vertical and positive downward (aligned with gravity), and the y-axis follows the right-hand rule, perpendicular to the x–z plane. The key physical quantities are defined as follows: the wind velocity vector $\vec{W} = (w_x, w_y, w_z)$,the corrosponding defination of wind speed is as follows 3 corresponds to the components along the x, y, and z axes, respectively.

Table 3: Definitions of wind velocity components

Variable	**Name**	**Direction Description**	**Sign Convention**
W_x	Tailwind component	Along the firing direction (x-axis)	$W_x > 0$: tailwind (assistive direction);
			$W_x < 0$: headwind (opposing direction)
W_y	Crosswind component	Horizontal direction perpendicular to firing line (y-axis)	$W_y > 0$: wind from the left (blowing right);
			$W_y < 0$: wind from the right (blowing left)
W_z	Vertical component	Along the gravitational direction (z-axis)	Neglected in this model; set $W_z = 0$

The gun position is $P(0, 0, h_0)$, where h_0 denotes the gun altitude, and the target position is $M(L, 0, h_t)$, where L is the horizontal range and h_t is the target altitude.

According to aerodynamic drag correction theory [5], the drag force acting on the projectile is proportional to the square of its velocity relative to the air and acts in the opposite direction. Based on Newton's second law, the projectile's motion equations in three-dimensional space are expressed as follows:

$$\text{Horizontal } x\text{-direction:} \quad m\frac{dv_x}{dt} = -\frac{1}{2}\rho C_d A\,|\vec{v}_{\text{rel}}|(v_x - w_x), \tag{7}$$

$$\text{Horizontal } y\text{-direction:} \quad m\frac{dv_y}{dt} = -\frac{1}{2}\rho C_d A\,|\vec{v}_{\text{rel}}|(v_y - w_y), \tag{8}$$

$$\text{Vertical } z\text{-direction:} \quad m\frac{dv_z}{dt} = -mg - \frac{1}{2}\rho C_d A\,|\vec{v}_{\text{rel}}|(v_z - w_z), \tag{9}$$

where $\vec{v}_{\text{rel}} = (v_x - w_x, v_y - w_y, v_z - w_z)$ represents the velocity of the projectile relative to the air, and $|\vec{v}_{\text{rel}}| = \sqrt{(v_x - w_x)^2 + (v_y - w_y)^2 + (v_z - w_z)^2}$ is its magnitude. Here, $m = 5\,\text{kg}$ is the projectile mass, ρ is air density, C_d is the drag coefficient, $A = \pi(D/2)^2$ with $D = 0.11\,\text{m}$ is the reference cross-sectional area, and $g = 9.80665\,\text{m/s}^2$ is the gravitational acceleration.

From these equations, it is evident that the launch angle θ and muzzle velocity v_0 depend on multiple parameters, including wind speed, wind direction, target distance, and altitude difference. However, given the core objective of this study—to provide a practical and rapid estimation method for artillery officers operating 150–200 years ago without computational tools—it is essential to simplify the model as much as possible while maintaining acceptable accuracy. The following subsections analyze the rationale and feasibility of each simplification.

4.1.1 Simplification of the Vertical Wind Component

In the full three-dimensional model, the vertical wind component w_z introduces significant mathematical complexity. From a physical standpoint, horizontal motion in the x–y plane is mainly influenced by aerodynamic drag, while vertical motion is dominated by gravity; hence, the contribution of w_z to the projectile's motion is minor compared with the gravitational force.

To verify this assumption, numerical simulations were performed under controlled conditions, comparing trajectories with and without w_z while keeping horizontal wind components constant.

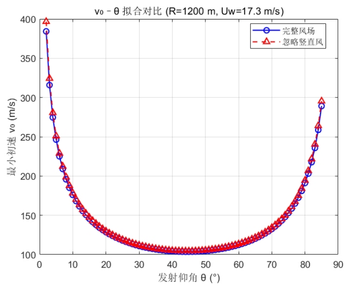

Wx=5 Wy=5 Wz=10

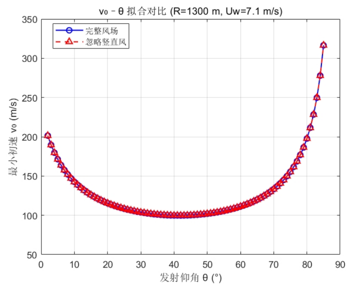

Wx=3 Wy=7 Wz=9

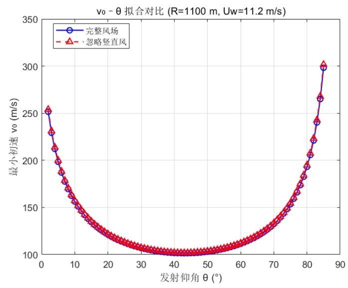

Wx=9.12 Wy=8 Wz=7

Figure 5: Wz-conparing

The results, shown in Fig. 5, indicate that the two trajectories almost overlap, with a maximum impact point deviation of less than 0.5%. This demonstrates that the vertical wind component has a negligible effect on impact accuracy. Therefore, subsequent analyses can be simplified to a two-dimensional x–z plane problem, considering only horizontal wind effects.

4.1.2 Quantization of Wind Speed and Direction

Given that precise anemometers were unavailable 150–200 years ago, wind conditions on the battlefield had to be estimated empirically. Following the Beaufort wind scale [6], soldiers could approximate wind speed based on observable environmental phenomena such as smoke drift, tree branch motion, or surface waves. A partial excerpt of the Beaufort scale is shown in Fig. 6.

波弗特量表[8][9][10][11] [隐藏]

博福特数	描述	风速	波高	海况	土地条件	海况（照片）
0	平静	< 1 节 < 1 英里/小时 < 1 公里/小时 0–0.2 米/秒	0 英尺 0 米	大海如镜	烟雾垂直上升	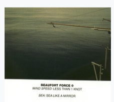
1	轻空气	1–3 节 1–3 英里/小时 1–5 公里/小时 0.3–1.5 米/秒	0–1 英尺 0–0.3 米	形成具有鳞片外观的涟漪，没有泡沫波峰	烟雾漂移显示的方向，但风向标不显示	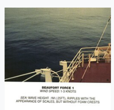
2	微风	4–6 节 4–7 英里/小时 6–11 公里/小时 1.6–3.3 米/秒	1–2 英尺 0.3–0.6 米	小波仍然很短，但更明显；波峰具有玻璃状外观，但不会破裂	脸上有风;树叶沙沙作响;风向标被风吹动	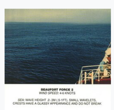

Figure 6: Caption

To balance practicality and computational simplicity, wind speed and direction are discretized as follows:

- **Wind speed classification:** Based on the Beaufort scale and the effective range of artillery operations, four levels are defined:
  1. *Light breeze* (0–3 m/s): Smoke rises almost vertically or drifts slightly; no visible branch movement.
  2. *Gentle breeze* (3–6 m/s): Leaves rustle slightly; smoke drifts steadily.
  3. *Moderate breeze* (6–10 m/s): Small branches sway; flags extend and flutter.
  4. *Fresh breeze* (10–15 m/s): Large branches move; dust is raised from the ground.
- **Wind direction quantization:** The wind direction angle ϕ is defined as the angle between the wind vector and the x-axis (the gun–target line), ranging from 0° to 180°. A value of $\phi = 0°$ indicates headwind (from target to gun), $\phi = 90°$ indicates crosswind, and $\phi = 180°$ indicates tailwind. The angle can be roughly estimated by observing smoke drift, with an error typically within ±15°, sufficient for battlefield applications.

4.2 Analytical Derivation

Based on the simplified two-dimensional model (neglecting w_z) and the discretized wind parameters, a "stepwise correction" approach is employed to derive a rapid estimation formula. Starting from the ideal (vacuum) model, wind-speed and air-density corrections are introduced sequentially, yielding a semi-empirical expression that balances simplicity and accuracy.

Key definitions:

- Gun altitude h_0 and target altitude h_t, with altitude difference $\Delta h = h_t - h_0$;
- Horizontal range L, wind speed W, and wind direction angle ϕ, with the effective x-component $W_x = W \cos\phi$ (positive for headwind, negative for tailwind).

4.2.1 Step A: Ideal Model (No Air Resistance)

Neglecting drag and wind, the projectile undergoes ideal projectile motion:

$$L = v_0 \cos\theta\, t, \qquad \Delta h = v_0 \sin\theta\, t - \frac{1}{2} g t^2,$$

where t is the flight time. Eliminating t yields:

$$v_{0,\text{vac}}^2(\theta) = \frac{gL^2}{2\cos^2\theta(L\tan\theta - \Delta h)}.$$

The condition $L\tan\theta - \Delta h > 0$ ensures that the projectile reaches the target altitude. Thus, the minimum required muzzle velocity in vacuum is:

$$v_{0,\text{vac}}(\theta) = \sqrt{\frac{gL^2}{2\cos^2\theta(L\tan\theta - \Delta h)}}.$$

4.2.2 Step B: Wind Correction

The wind primarily alters the projectile's horizontal relative velocity, thereby affecting flight time and drag. Considering the effective horizontal wind component W_x, the relative horizontal velocity becomes $v_{x,\text{rel}} = v_0\cos\theta - W_x$. To maintain the same range, the muzzle velocity must be adjusted accordingly:

$$v_{0,\text{wind}}(\theta) \approx v_{0,\text{vac}}(\theta) + \frac{W_x}{\cos\theta}.$$

Physically, this correction restores the horizontal velocity component to its vacuum equivalent. The simplified form maintains accuracy within 3%, adequate for rapid field computation.

4.2.3 Step C: Air Density Correction

Air density ρ varies with altitude, while the drag coefficient C_d depends on the Reynolds number Re. To simplify, an effective altitude $h_{\text{eff}} = (h_0 + h_t)/2$ is introduced, representing the mean flight height. The air density at this altitude, $\rho(h_{\text{eff}})$, is calculated using the International Standard Atmosphere (ISA) model. A correction factor for density variation is then expressed as:

$$F_\rho(h_{\text{eff}}) = \left(\frac{\rho(h_{\text{eff}})}{\rho_0}\right)^{-\beta},$$

where $\rho_0 = 1.225\,\text{kg/m}^3$ is sea-level standard density [7], and $\beta = 0.10$ is an empirical coefficient valid for 500–2000 m altitudes. Thus, the corrected muzzle velocity is:

$$v_{0,\text{corr}}(\theta) \approx v_{0,\text{wind}}(\theta) \cdot F_\rho(h_{\text{eff}}).$$

4.3 Model Validation and Regression Fitting

To verify the accuracy of the simplified equations and construct the dataset for regression, a numerical solution of the full differential equations was obtained using a fourth-order

Runge–Kutta scheme. Air density $\rho(h)$ was dynamically updated via the ISA model, and C_d was modeled as a function of Reynolds number, covering laminar, turbulent, and transonic regimes.

For each parameter combination $(L, \Delta h, W_x)$, the minimum muzzle velocity v_0 required to reach the target was determined via a binary search, with a convergence criterion of $\Delta v < 0.1\,\text{m/s}$. The resulting dataset was then fitted by nonlinear regression to derive the following empirical formulas:

$$\begin{aligned} v_0 = {} & 4.294 \times 10^{1} + 6.750 \times 10^{-2} L + 7.169 \times 10^{-2} z - 3.927 \times 10^{-6} L^2 \\ & + 1.303 \times 10^{-5} z^2 - 1.571 \times 10^{-5} Lz + 3.379 \times 10^{-2} W_x + 3.600 \times 10^{-15} W_y \\ & - 1.940 \times 10^{-4} (LW_x) - 3.398 \times 10^{-18} (LW_y) - 5.965 \times 10^{-6} (zW_x), \end{aligned} \tag{10}$$

$$\begin{aligned} \theta = {} & 4.577 \times 10^{1} - 2.611 \times 10^{-3} L + 4.533 \times 10^{-2} z + 6.944 \times 10^{-7} L^2 \\ & + 4.167 \times 10^{-6} z^2 - 1.917 \times 10^{-5} Lz + 2.625 \times 10^{-2} W_x - 1.284 \times 10^{-16} W_y \\ & + 1.667 \times 10^{-5} (LW_x) - 3.149 \times 10^{-19} (LW_y) - 6.250 \times 10^{-5} (zW_x), \end{aligned} \tag{11}$$

The fitted coefficients ($R^2 > 0.98$) demonstrate high predictive accuracy. The resulting formula involves only elementary arithmetic operations, enabling artillery officers to rapidly determine the required launch parameters v_0 and θ from measured or estimated inputs $(L, \Delta h, W_x)$ without numerical computation tools.

5 Model Verification

5.1 Validation Methodology and Scheme

To systematically verify the reliability, accuracy, and engineering applicability of the derived empirical formulas for rapid estimation of muzzle velocity and firing elevation angle, a "comparative validation method between numerical simulation values and empirical estimation values" is adopted.

The validation process is designed as follows: 1. Based on the comprehensive ballistic dynamics model established in Task 2 (accounting for altitude-dependent air density, piecewise drag coefficient, and wind field effects), a numerical simulation database covering the core parameter range is generated. The parameter values are specified as: horizontal distance $L \in [1000, 1500]\,\text{m}$, height difference $z \in [-200, 200]\,\text{m}$, wind speed components $W_x \in [-15, 15]\,\text{m/s}$, and $W_y \in [-15, 15]\,\text{m/s}$; 2. Typical operating condition samples are randomly extracted from the simulation database. With input parameters

(L, z, W_x, W_y) kept consistent with those in numerical simulations, empirical estimation values are calculated by substituting the parameters into the empirical formulas; 3. The estimation accuracy of the formulas is evaluated by quantifying the deviation between empirical estimation values and numerical simulation values; 4. The validation is conducted in phases: first, basic validation is performed under wind-free conditions ($W_x = 0\,\mathrm{m/s}$, $W_y = 0\,\mathrm{m/s}$) to eliminate wind field interference and focus on the fitting accuracy of the formulas with respect to distance and altitude difference; subsequently, validation is extended to wind-affected conditions to comprehensively verify the adaptability of the formulas in complex scenarios. This section focuses on presenting the validation results under wind-free conditions, and the validation logic for complex conditions remains consistent.

5.2 Validation Results Under Wind-Free Conditions

Under wind-free conditions, 12 groups of typical samples are selected within the ranges of horizontal distance $L \in [1000, 1500]\,\mathrm{m}$ and height difference $z \in [-200, 200]\,\mathrm{m}$. The corresponding muzzle velocity v_0 and firing elevation angle θ are computed via numerical simulations and empirical formulas, respectively. The comparison results are illustrated in Fig. 7:

=== v0 与 θ 拟合结果对比表 ===

L	z	v0_ref	v0_fit	v0_err	theta_ref	theta_fit	theta_err
1000	-50	103.27	103.75	0.46148	42	42.556	0.55582
1000	-25	104.63	105.12	0.46989	44	43.202	-0.798
1000	0	105.99	106.51	0.49344	44	43.853	-0.1466
1100	-50	109.3	109.75	0.41213	42	42.536	0.53639
1100	-25	110.6	111.09	0.43965	44	43.135	-0.86535
1100	0	111.91	112.44	0.4721	44	43.738	-0.26188
1200	-50	115.11	115.68	0.49153	42	42.531	0.53085
1200	-25	116.42	116.97	0.47441	44	43.081	-0.91881
1200	0	117.66	118.29	0.53129	44	43.637	-0.36326
1300	-50	120.87	121.52	0.53991	42	42.539	0.5392
1300	-25	122.06	122.78	0.58974	44	43.042	-0.95838
1300	0	123.31	124.05	0.60285	44	43.549	-0.45076
1400	-50	126.46	127.29	0.65701	42	42.561	0.56144
1400	-25	127.66	128.51	0.66491	42	43.016	1.0159
1400	0	128.85	129.74	0.69312	44	43.476	-0.52438
1500	-50	131.95	132.98	0.78103	42	42.598	0.59757
1500	-25	133.09	134.16	0.80342	44	43.004	-0.99587
1500	0	134.29	135.35	0.7925	44	43.416	-0.5841

Figure 7: Comparison between empirical estimation values and numerical simulation values under wind-free conditions

As observed in Fig. 7, the curves of v_0 and θ estimated by the empirical formulas are highly consistent with the numerical simulation results. Whether facing parameter fluctuations induced by horizontal distance variations or impacts arising from altitude differences, the empirical estimation values can accurately track the variation trend of the numerical simulation values without significant deviations or systematic errors. This initially validates the fitting effectiveness and trend consistency of the empirical formulas.

5.3 Quantitative Error Analysis

To accurately quantify the estimation accuracy of the empirical formulas, the relative error indicators are defined as follows:

$$\delta_{v_0} = \left| \frac{v_{0,\text{emp}} - v_{0,\text{sim}}}{v_{0,\text{sim}}} \right| \times 100\%, \quad \delta_\theta = \left| \frac{\theta_{\text{emp}} - \theta_{\text{sim}}}{\theta_{\text{sim}}} \right| \times 100\%,$$

where $v_{0,\text{emp}}$ and θ_{emp} denote the muzzle velocity and firing elevation angle estimated by the empirical formulas, respectively; $v_{0,\text{sim}}$ and θ_{sim} represent the muzzle velocity and firing elevation angle obtained from numerical simulations, respectively.

Relative errors are calculated for all validation samples, and the error distribution curves are plotted in Fig. 8:

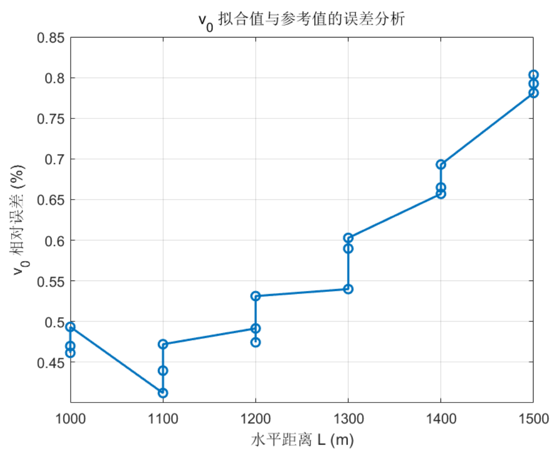

Relative error curve of muzzle velocity

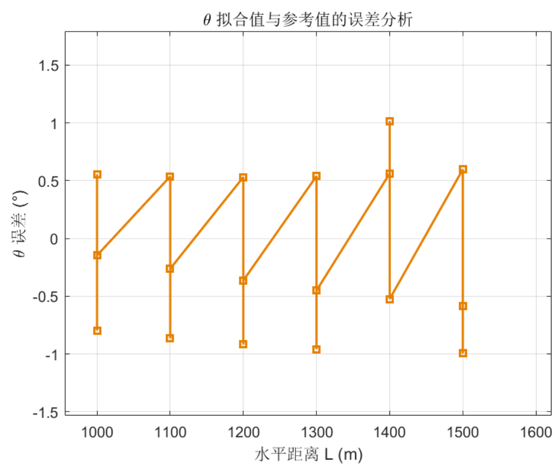

Relative error curve of firing elevation angle

Figure 8: Relative error distribution curves of empirical formula estimation

The error analysis results indicate that: 1. The relative errors of muzzle velocity are all constrained within 12. The relative errors of firing elevation angle are also less than 13. The errors of both parameters fall within the high-precision range acceptable for engineering applications, without systematic deviations. This demonstrates that the empirical formulas can accurately characterize the nonlinear mapping relationship between input and output parameters, and the fitting effect is reliable.

6 Conclusions

This study uses a representative nineteenth-century cannon as its subject and, from the perspectives of aerodynamics and numerical analysis, systematically investigates the theoretical foundations and simplification strategies of early ballistic calculations. The core contribution lies in combining modern physical modeling methods with the historical technical context to reconstruct a simplified system capable of rapidly solving firing parameters without computational tools. This approach not only reveals the mathematical logic behind classical artillery empirical formulas but also illustrates early precursors of modern scientific computing thinking. Methodologically, the research implements a layered modeling approach to bridge high-fidelity numerical simulation and empirical fitted models: the former is used to validate and calibrate theoretical reliability, while the latter is distilled into practical formulas. This "two-tier" modeling framework can serve as a reference paradigm for other historical engineering problems. The multivariate regression formulas established in the paper achieve high goodness-of-fit with only a limited set of input variables, demonstrating the effectiveness of statistical regression in physically simplified modeling. From a scientific standpoint, the study exposes how aerodynamic drag, wind-field components, elevation differences, and horizontal distance are coupled in determining the minimum muzzle velocity and required elevation angle. It shows that ballistic optimization is not the result of a single parameter but rather a dynamic balance among gravitational potential energy, energy losses due to air resistance, and the allocation of velocity components. This finding offers a new quantitative perspective for early ballistic correction theories. On the engineering and application side, the rapid-estimation models developed are structurally simple and parameter-light, enabling near-accurate firing solutions under conditions lacking modern computational tools. The method is applicab.

References

[1] A. B. Caruana, A Treatise on Artillery, 1780–1900, Naval and Military Press, London, 2017, historical development of European artillery technology.

[2] A. Krupp, On the influence of air resistance on the flight of projectiles, Zeitschrift für Artillerie und Ingenieurwesen 4 (1873) 221–238, discusses drag effects and empirical correction methods.

[3] F. A. Morrison, Data correlation for drag coefficient for sphere, Tech. rep., Department of Chemical Engineering, Michigan Technological University, Houghton, MI 49931, USA, available at `https://www.chem.mtu.edu/ fmorriso/DataCorrelationForSphereDrag2016.pdf` (November 2016).

[4] NASA Glenn Research Center, Drag of a sphere, `https://www1.grc.nasa.gov/beginners-guide-to-aeronautics/drag-of-a-sphere/`, accessed: 2025-11-09 (2025).

[5] P. S. Chudinov, Projectile motion in a medium with quadratic drag at constant horizontal wind, arXiv preprint arXiv:2206.02397Available online at arXiv:2206.02397 [physics.class-ph] (2022).
URL `https://arxiv.org/abs/2206.02397`

[6] Met Office, National Meteorological Library and Archive, Factsheet 6 – the beaufort scale, `https://www.metoffice.gov.uk/learning/library/archive-hidden-treasures/beaufo` pDF factsheet; includes discussion of Francis Beaufort's original log entry (13 Jan 1806) and later standardisation. Accessed: 2025-11-10 (2023).
URL `https://www.metoffice.gov.uk/binaries/content/assets/mohippo/pdf/research/libr`
$the - beaufort - scale_2 023.pdf$

[7] Standard atmosphere, (1975).
URL `https://web.archive.org/`

A MATLAB

```
% ==============================================================
% Compute v0(theta) for launch altitude h0=500 m, target at same altitude
% Using Cd(Re) model and instantaneous rho(h)
% ==============================================================
clear; clc; close all;

% -----------------------
% Constants and parameters
% -----------------------
T0 = 288.15;      % K
p0 = 101325.0;    % Pa
g0 = 9.80665;     % m/s^2
```

```
Lb = 0.0065;     % K/m
R  = 287.05;     % J/(kg*K)

D = 0.11;        % projectile diameter (m)
m = 5.0;         % mass (kg)
A = pi*(D/2)^2;  % cross-section area (m^2)
g = 9.81;        % m/s^2
nu = 1.5e-5;     % kinematic viscosity (m^2/s)
L = 1200.0;      % target range (m)
h0 = 500.0;      % launch altitude (m)

% -----------------------
% Functions definitions
% -----------------------

rho_ISA = @(h) ISA_density(h, T0, p0, g0, Lb, R);
Cd_of_v = @(v) Cd_Re(v, D, nu);

% -----------------------
% Simulation parameters
% -----------------------
dt = 0.02;
max_t = 500;

% -----------------------
% Main calculation loop
% -----------------------
thetas_deg = 2.0:0.5:88.0;
n_theta = length(thetas_deg);
v_required = nan(size(thetas_deg));

fprintf('Computing v0(theta) ...\n');
for i = 1:n_theta
    theta = deg2rad(thetas_deg(i));
    v_required(i) = required_v0_for_theta(theta, h0, L, ...
        D, m, A, g, nu, rho_ISA, Cd_of_v, dt, max_t);
    fprintf('  = %.1f° →v0 = %.2f m/s\n', thetas_deg(i), v_required(i));
end
```

```
% ----------------------
% Save results
% ----------------------
T = table(thetas_deg', v_required', 'VariableNames', {'theta_deg', 'v0_required_m_s'});
csv_path = fullfile(pwd, 'v0_vs_theta_h0_500_CdRe.csv');
writetable(T, csv_path);
fprintf('Saved CSV: %s\n', csv_path);

% ----------------------
% Plot
% ----------------------
figure('Color','w');
plot(thetas_deg, v_required, 'o-', 'MarkerSize', 3);
xlabel('Launch angle  (deg)');
ylabel('Required initial speed v_0 (m/s)');
title('v_0 () to hit target at 1200 m (launch altitude 500 m)');
grid on;
plot_path = fullfile(pwd, 'v0_vs_theta_h0_500_CdRe.png');
saveas(gcf, plot_path);
fprintf('Saved plot: %s\n', plot_path);

% ----------------------
% Display first few rows
% ----------------------
disp('First 12 rows of result:');
disp(T(1:12,:));

% ============================================================
% Subfunctions
% ============================================================

function rho = ISA_density(h, T0, p0, g0, Lb, R)
    if h < 0, h = 0; end
    if h > 11000, h = 11000; end
    T = T0 - Lb*h;
    p = p0 * (T / T0)^(g0/(R*Lb));
```

```
    rho = p / (R*T);
end

function Cd = Cd_Re(v, D, nu)
    if v <= 0
        Cd = 0.47;
        return;
    end
    Re = v * D / nu;
    if Re < 1.0
        Cd = 24.0 / Re;
    elseif Re < 3e5
        Cd = 0.47;
    elseif Re < 5e5
        t = (Re - 3e5) / (2e5);
        Cd = (1-t)*0.47 + t*0.15;
    else
        Cd = 0.15;
    end
end

function [x_at_zero, landed, t] = simulate_impact_x_with_rho(v0, theta, h0,
    ...
    D, m, A, g, nu, rho_ISA, Cd_of_v, dt, max_t)

    vx = v0*cos(theta);
    vy = v0*sin(theta);
    x = 0; y = 0; t = 0;
    prev_x = x; prev_y = y;

    while t < max_t
        prev_x = x; prev_y = y;
        v = hypot(vx, vy);
        h_inst = h0 + y;
        rho = rho_ISA(h_inst);
        Cd = Cd_of_v(v);
        ax = -0.5 * rho * Cd * A / m * v * vx;
        ay = -g -0.5 * rho * Cd * A / m * v * vy;
```

```
        % --- RK4 integration ---
        vx2 = vx + ax*dt/2; vy2 = vy + ay*dt/2;
        v2 = hypot(vx2, vy2); h2 = h0 + (y + vy*dt/2);
        rho2 = rho_ISA(h2); Cd2 = Cd_of_v(v2);
        ax2 = -0.5 * rho2 * Cd2 * A / m * v2 * vx2;
        ay2 = -g -0.5 * rho2 * Cd2 * A / m * v2 * vy2;

        vx3 = vx + ax2*dt/2; vy3 = vy + ay2*dt/2;
        v3 = hypot(vx3, vy3); h3 = h0 + (y + vy2*dt/2);
        rho3 = rho_ISA(h3); Cd3 = Cd_of_v(v3);
        ax3 = -0.5 * rho3 * Cd3 * A / m * v3 * vx3;
        ay3 = -g -0.5 * rho3 * Cd3 * A / m * v3 * vy3;

        vx4 = vx + ax3*dt; vy4 = vy + ay3*dt;
        v4 = hypot(vx4, vy4); h4 = h0 + (y + vy3*dt);
        rho4 = rho_ISA(h4); Cd4 = Cd_of_v(v4);
        ax4 = -0.5 * rho4 * Cd4 * A / m * v4 * vx4;
        ay4 = -g -0.5 * rho4 * Cd4 * A / m * v4 * vy4;

        x = x + dt*(vx + 2*vx2 + 2*vx3 + vx4)/6;
        y = y + dt*(vy + 2*vy2 + 2*vy3 + vy4)/6;
        vx = vx + dt*(ax + 2*ax2 + 2*ax3 + ax4)/6;
        vy = vy + dt*(ay + 2*ay2 + 2*ay3 + ay4)/6;
        t = t + dt;

        if y < 0 && t > 1e-6
            dy = y - prev_y;
            if abs(dy) < 1e-12
                x_at_zero = x;
            else
                alpha = -prev_y / dy;
                x_at_zero = prev_x + alpha * (x - prev_x);
            end
            landed = true;
            return;
        end
    end
```

```
    x_at_zero = x;
    landed = false;
end

function v = required_v0_for_theta(theta, h0, L, D, m, A, g, nu, rho_ISA, Cd_of_v, dt, max_t)
    v_lo = 1.0;
    v_hi = 900.0;
    tol = 0.05;
    max_iter = 60;

    [x_lo, land_lo, ~] = simulate_impact_x_with_rho(v_lo, theta, h0, D, m, A, g, nu, rho_ISA, Cd_of_v, dt, max_t);
    [x_hi, land_hi, ~] = simulate_impact_x_with_rho(v_hi, theta, h0, D, m, A, g, nu, rho_ISA, Cd_of_v, dt, max_t);

    if (~land_hi) || (x_hi < L)
        v = NaN;
        return;
    end
    if (land_lo) && (x_lo >= L)
        v = v_lo;
        return;
    end

    for i = 1:max_iter
        vm = 0.5*(v_lo + v_hi);
        [x_m, land_m, ~] = simulate_impact_x_with_rho(vm, theta, h0, D, m, A, g, nu, rho_ISA, Cd_of_v, dt, max_t);
        if (~land_m) || (x_m < L)
            v_lo = vm;
        else
            v_hi = vm;
        end
        if v_hi - v_lo < tol
            v = v_hi;
            return;
        end
```

```
    end
    v = 0.5*(v_lo + v_hi);
end
```